

# Quantification of Liquid Water Saturation in a Transparent Single-Serpentine Cathode Flow Channel of PEM Fuel Cell by Using Image Processing

S. Nirunsin\* and Y. Khunatorn

Department of Mechanical Engineering, Chiang Mai University, Chiang Mai, Thailand  
\*Corresponding Author: nirunsin@hotmail.com, Tel. (66)53-944146, Fax. (66)53-944145

**Abstract:** The objective of this research is to quantify the water content on the cathode side in various PEM fuel cell operations. It can be revealed by direct visualization in an operational transparent single-serpentine PEM fuel cell. Images of liquid water accumulated inside the cathode flow channel were recorded by a digital camera to study water flooding in PEM fuel cell. The water coverage area in the cathode flow channel was estimated by an image processing technique. The effects of oxygen flow rate, cell temperature and time development on the water flooding were studied. The results indicated that excessive low or high cell temperature caused water to flood into the PEM fuel cell. The increasing of oxygen flow rate can remove more liquid water out of the cathode flow channel. However, too high oxygen flow rate caused the insufficient water content to maintain the membrane in the hydrated state and the dramatic decrease of fuel cell's performance. The water flooding did not appear in a single-serpentine cathode flow channel when a transparent PEM fuel cell has operated within 40 minutes.

**Keywords:** PEM fuel cell; water management; direct visualization; transparent single-serpentine, image processing.

## 1. Introduction

Fuel cells are presently regarded as promising energy conversion systems for electrical vehicles and power stations. PEM fuel cells, in particular, have many advantages, such as using solid polymer electrolytes, low operating temperatures, cold start-up, high energy efficiency and power density [1-3]. The polymer membrane in a PEM fuel cell should be in a hydrated state to facilitate proton transport across the membrane. If there is not enough water, the membrane becomes dry and its resistance increases sharply. However, if too much water is present, flooding may occur, which blocks the transport of reactants to the reaction sites. Thus, water management in PEM fuel cells is very important and has been mentioned in many studies [3]. In a PEM fuel cell, the water distribution in the membrane is determined by two main mechanisms: electro-osmotic drag and diffusion. In practice, there is much more water resulting in flooding in the cathode than in the anode, especially at high current density and low temperature conditions. If the generated water is not removed from the electrode and flow channels at a sufficient rate, flooding appears and the transport of reactants is hindered [4]. Many studies on water transfer and water management have been published. There are several models that can predict PEM's performance based on differences in the level of water flooding [5-7]. Even though there have been new developments in self-humidifying polymer electrolyte membranes which can hydrate a PEM fuel cell by generating water from the electrochemical reaction [8-9]. However, these studies did not present the images and patterns of the liquid water in PEM fuel cell.

At present, there are many techniques to detect cathode flooding. One can use global tools, such as fully saturated air at the exit and increasing the pressure drop. Flooding is also associated with a fuel cell's performance. Local information about flooding can be given by current and temperature distribution measurements [10]. Physical indicators of flooding, such as current, temperature, pressure drop and relative humidity are also tools to detect water flooding in a fuel cell. Various imaging techniques can be used to investigate two-phase flow dynamics inside a fuel cell. These techniques are direct visualization [11-15], neutron radiography [16], X-ray micro tomography [17] and magnetic resonance imaging [18]. Although direct visualization requires a special cell design, it is very attractive experimental technique as visual information offers the advantage of studying the two-

phase phenomena at different levels of operating condition on water distribution and water flooding in PEM fuel cells [12]. However, the visualization primarily provides qualitative data and there have been only a few reports about quantifying the water content through this technique [11].

The purpose of this paper is to quantify the accumulated water in a transparent single-serpentine cathode flow channel. The effects of cell temperature, cathode gas flow rate and time development on the water flooding were also examined. The water images were recorded by digital camera. Since the digital images presented two-dimensional information, the water content in this paper must be measured in terms of water coverage area which can be quantified by using image processing technique.

## 2. Image processing

A digital image is defined as a two-dimensional function,  $f(x,y)$ , where  $x$  and  $y$  are spatial coordinates, and the amplitude of  $f$  at any pair of coordinates  $(x,y)$  is the intensity or gray level (0-255) of the image at that point. A digital image is composed of a finite number of elements, each of which has a particular location and gray level value. These elements are referred to as image elements or pixels. Pixel is the term most widely used to denote the elements of a digital image. The digital image can be considered as a large array of pixels. Thus, the digital image can be manipulated with matrix operations in image processing routines to evaluate any important information.

The amount of water in the cathode flow channel of a PEM fuel cell can be quantified by using an image processing routine. The water appearance in the cathode flow channel was represented by the water pixels in the spatial domain of the digital image. The water image  $W(x,y)$  was separated from background image  $I_r(x,y)$  by subtracting the image of reaction state  $I_r(x,y)$  described in Eq. (1) from dry state image  $I_d(x,y)$  in Eq. (2). The calculation of water content from the images may be written as the following equations.

$$I_d(x,y) = I(x,y) + \eta_d(x,y), \quad (1)$$

$$I_r(x,y) = I(x,y) + W(x,y) + \eta_r(x,y), \quad (2)$$

$$W(x,y) = I_r(x,y) - I_d(x,y) + (\eta_d(x,y) - \eta_r(x,y)) \quad (3)$$

where  $\eta_d(x, y)$  and  $\eta_r(x, y)$  are noise functions of the dry and reaction states, respectively. These may be occurred from reflection and disturbance of light source frequency (50 Hz). However, the term of noise function in Eq. (3) may be negligible because the subtraction of both noise functions is very small. So that Eq. (3) can be rewritten as Eq. (4) without the term for noise function.

$$W(x, y) = I_r(x, y) - I_d(x, y) \quad (4)$$

The number of water pixels in Eq. (4) can be determined by using a histogram of the image  $W(x, y)$ . The histogram is a graph indicating the number of times each gray level occurs in the image. The probability density of water pixels  $P_w(k)$  can be obtained by normalized histogram with dividing all water pixels  $n_k$  by the total number of pixels  $n$  in the image as showed in Eq. (5).

$$P_w(k) = \frac{n_k}{n} \quad (5)$$

where  $k$  is gray level of water. Therefore, the water coverage area  $A_w$  on the cathode side can be quantified from the image by multiplication of  $P_w(k)$  with active area size of  $A_c$ .

$$A_w = A_c \times P_w(k) \quad (6)$$

However, the capable water coverage area is only a part of gas flow field channel area which dose not includes the ribs area. Therefore, from a single-serpentine flow field design of cathode side, the maximum area is covered by water about 55 percent of the whole active area.

The brass plate was machined as a gas flow field plate in the cathode side and conventional graphite was used as a gas flow field plate in the anode side. Transparent acrylic with thickness of 15 mm was used as the end plate at the cathode side. Membrane electrode assembly (MEA) was made form Gore in 5612 series. There was  $0.6 \text{ mg/cm}^2$  at cathode and  $0.4 \text{ mg/cm}^2$  at anode. The membrane thickness was  $25 \mu\text{m}$ . The size of physical active area was  $25 \text{ cm}^2$ . When the machined brass plate was assembled between the transparent acrylic and MEA, the 3M 468MP adhesive film was used as sealing strip between the flow field channel and the transparent acrylic to obstruct the gas cross over the ribs and leak out from the cathode active area. A transparent window was set up in the cathode clamping plate so that we were able to investigate the water build-up and flooding inside the PEM fuel cell as shown in Fig. 2. Two circle electrical heater pads were attached on the anode end plate and cathode flow field plate. A temperature controller and temperature sensor were used to control the cell temperature.

### 3. Experimental

A transparent PEM fuel cell was designed in a single-serpentine flow channel (1.5 mm in channel width, 2 mm in depth and 1.5 in rib width). Fig. 1 shows the schematics drawing of the cathode side of a transparent PEM fuel cell.

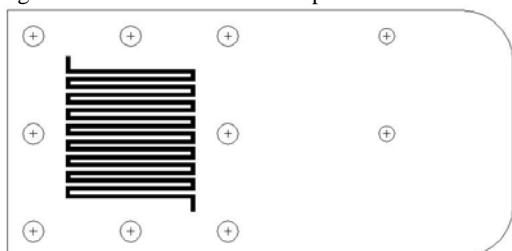


Figure 1. The schematic drawing of the cathode flow field plate.



Figure 2. A transparent single-serpentine PEM fuel cell.

Fig. 3 shows the experimental set-up. The experimental set-up consists of: (i) a fuel and oxidant reactant supply system; (ii) a fuel cell test system; (iii) a digital camera recording system. Pure hydrogen and oxygen were used as fuel and oxidant reactant, respectively.

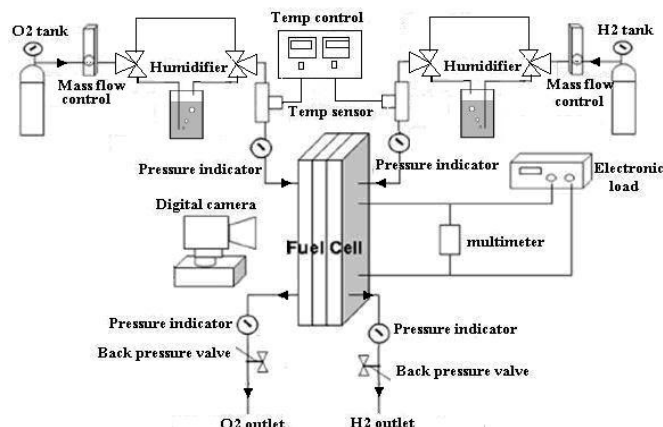


Figure 3. The diagram of experimental set-up in a transparent PEM fuel cell.

Both hydrogen and oxygen gas to the fuel cell were not humidified, so that the water that was observed in the cathode flow channel of a transparent fuel cell has been generated only by the electrochemical reaction. Gas flow rates were controlled by mass flow controllers (MKS, Type MB-100) with a precision of  $\pm 0.1\%$ . A nitrogen purge system was used to clean out the fuel and oxidant reactant left in the test system pipelines and fuel cells. The fuel cell current loading was controlled by electronic load (TDI, RBL448 Series). The water flooding in the cathode flow channel was recorded by digital camera (Cannon, GT10). During each experiment, the reaction area of the cathode side was first photographed in its dry state. Photographs were taken every 5 minutes after the fuel cell reaction occurred at a constant current loading of 5 A ( $200 \text{ mA/cm}^2$ ). In order to prevent the voltage of the fuel cell operation dropping too low, the current loading in this experiment must be lower than the normal operating current density ( $400\text{-}600 \text{ mA/cm}^2$ ) because the fuel cell was operated in a non-humidified state and the transparent configuration has more ohmic loss from metallic corrosion of the brass plate [19, 20] than does the conventional graphite configuration. The accuracy of using the image processing technique was achieved by disposition of all image components in the same frame reference and also under the same intensity of light sources. As a result, the subtraction image between the reaction's state image and dry state image allowed only the water image in the cathode flow channel. Finally, before changing the operating conditions, nitrogen gas was used to purge the gas flow channel to recondition it back to its dry state.

#### 4. Results and discussion

The water flooding images on the different fuel cell operating conditions were recorded by digital camera. Image processing was used to manipulate the digital images in this experiment. Fig. 4 (a) and 4 (b) show an example of the water image, which was manipulated by image processing techniques.

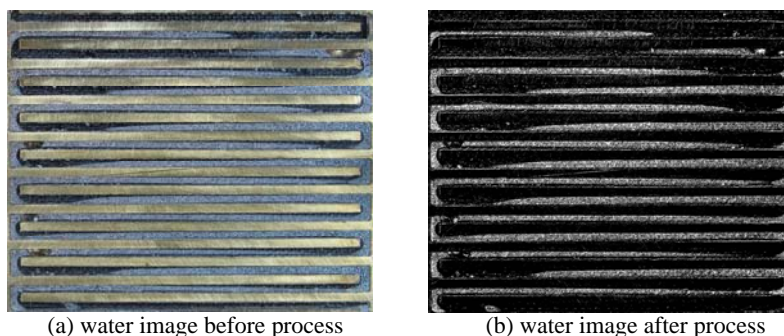
##### 4.1 The effect of cell temperature

The effect of cell temperature on a transparent PEM fuel cell has been described in other papers. However, most of them have analyzed this phenomenon with qualitative data only [11-13]. Fig. 5 shows the effect of cell temperature in the cathode flow channel. All images were recorded at 20 minutes after the fuel cell was loaded at a constant current of 5 A. A transparent fuel cell was operating at the conditions of atmosphere pressure, oxygen gas flow rate of 40 ml min<sup>-1</sup> (stoichiometric ratio of 2.18) and hydrogen flow rate of 60 ml min<sup>-1</sup> (stoichiometric ratio of 1.63). There was no external humidifier supplied to either side of the PEM fuel cell in order to ensure that any water was generated from the fuel cell reaction.

Fig. 5 shows that the liquid water in the flow channel at low temperature was much more than at high temperature. When the fuel cell operated at a temperature lower than 60°C, there was

a greater water coverage area in the cathode flow channel. The accumulated water inside a transparent fuel cell did not only reduce the cathode flow channel area and effective electrochemical reaction site, but it also obstructed mass transport. At the operating temperature, i.e. 25°C, the cell's performance would be low because the flow channel would be filled with the liquid water. By increasing the cell's temperature, the water coverage area in the flow channel was decreased according to the water quantified by image processing in Fig. 6.

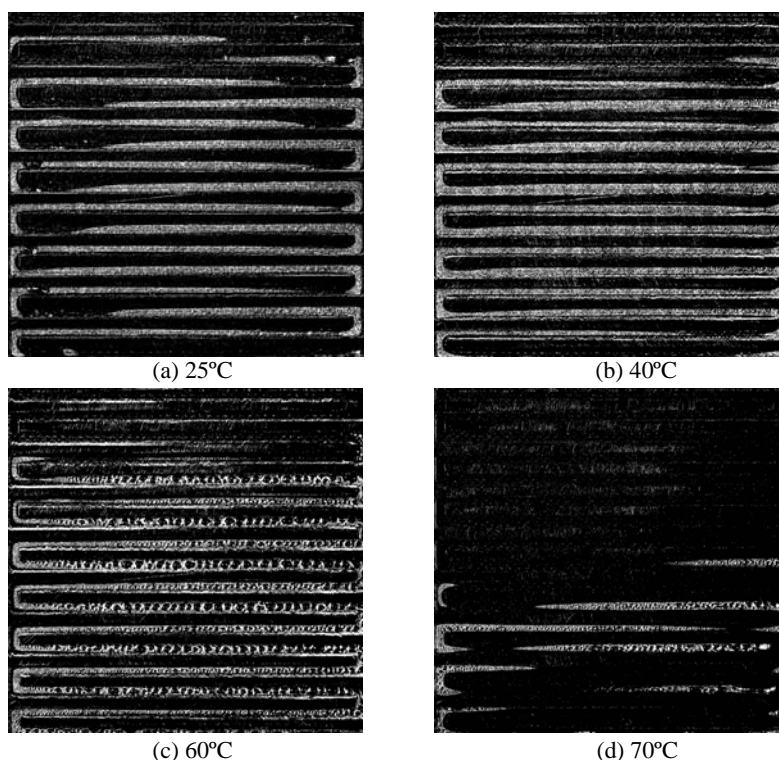
Interestingly, Fig. 6 shows the water coverage area at 25°C to be less than that at 40°C. The reason is that when the nitrogen gas was used to purge the accumulated liquid water in the cathode flow channel to recondition to the dry state before changing the temperature from 25°C to 40°C, there was a small amount of liquid water remaining in the gas diffusion layer (GDL). So, this water was added to the water product of the next fuel cell operating condition to raise the amount of water coverage area at 40°C higher than at 25°C. But, this phenomenon was less dominating at the higher operating temperature because the remaining liquid water had received more thermal energy from the heater of the temperature controller. So, more water vapor was generated, which would be more easily leave from the porous electrode, and drive faster out of the cathode flow channel before the electronic load was turned on to generate the



(a) water image before process

(b) water image after process

**Figure 4.** Example of water image manipulated by image processing technique.



(a) 25°C

(b) 40°C

(c) 60°C

(d) 70°C

**Figure 5.** Effect of cell temperature on water appearance in cathode flow channel.

electrochemical reaction and water product in the next cell temperature condition. As a result of the operating temperature rising, the vapor condensation rate was much slower than that at low temperature. There was only a little water in the cathode flow channel at the highest cell temperature of 70°C as shown in Fig. 6. In Fig. 7, when the cell temperature was increasing from 25°C to 60°C, the fuel cell's performance would be higher, but the water content began to decrease a little at temperature of 60°C because there was more water vapor generated in the cathode flow channel. The water content decreased rapidly at the highest temperature of 70°C. As the lowest content of water at 70°C, the membrane would become dry and its resistance would increase sharply, which gave the lowest performance. Therefore, the appropriate cell temperature would be in the range of 40–60°C, which provided the best fuel cell performance.

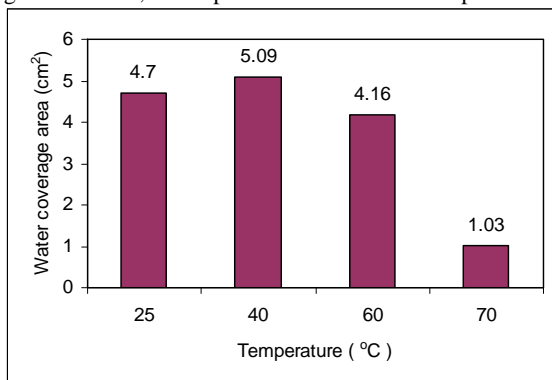
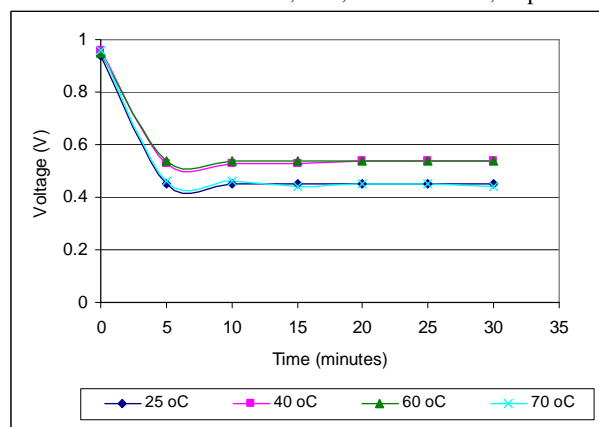


**Figure 6.** The water coverage area in cathode flow channel of difference cell temperatures.

This moderate range of cell temperature was also recommended by Liu et al. [13]. Water management problems, such as water flooding or membrane dehydration, can lead to a drop in cell's performance. Therefore, water management is important to fuel cell performance, which is also related to thermal management.

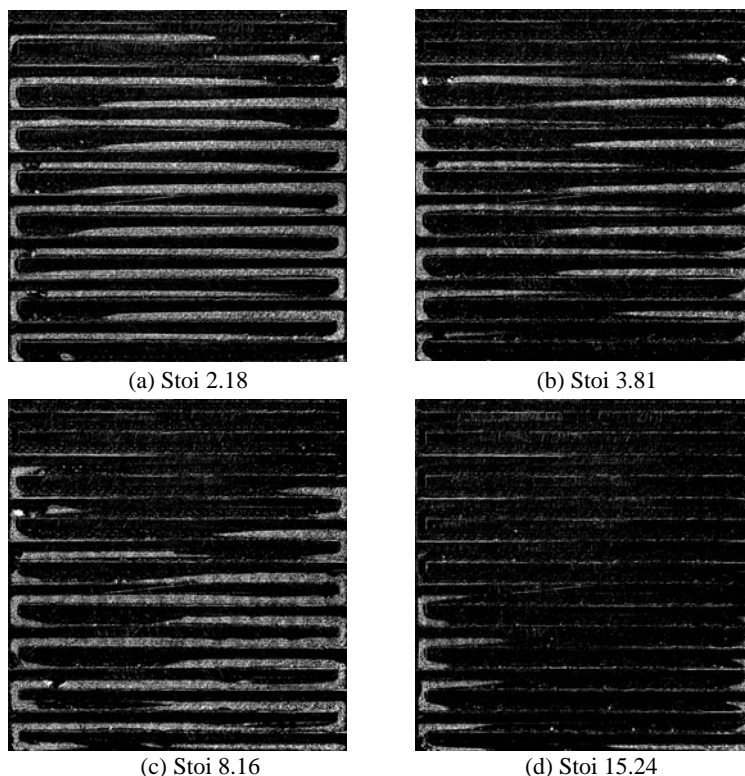
#### 4.2 The effect of oxygen flow rates

The cathode gas flow rate can contribute to water removal. In order to reduce the concentration losses from water flooding, the stoichiometric ratio must be at least 2 [21], but if the cathode reactant gas is in the fully hydrated state, the stoichiometric ratio must be more than 43 to avoid water flooding in the cathode gas flow channel [5]. In this study case, the oxygen gas was not humidified so that the lowest stoichiometric ratio was defined at higher than 2. Fig. 8 shows the images of condensation of liquid water in the cathode flow channel at different oxygen flow rates. These photos were taken at a current of 5 A after the fuel cell had operated for 20 minutes at the ambient pressure and cell temperature of 25°C. The oxygen flow rates were 40 ml min<sup>-1</sup>, 70 ml min<sup>-1</sup>, 150 ml min<sup>-1</sup> and 280 ml min<sup>-1</sup>, and accordingly, the stoichiometric ratios were 2.18, 3.81, 8.16 and 15.24, respectively.



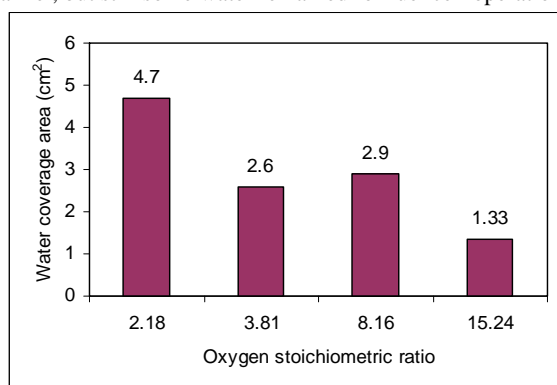
**Figure 7.** The cell voltage in difference cell temperatures at a constant current loading of 5 A.

When the stoichiometric ratio of oxygen was increased from 2.18 to 3.81, the water content in the cathode flow channel decreased to almost fifty percent and trended to more decrease in the oxygen stoichiometric ratio higher than 3.81 as shown in



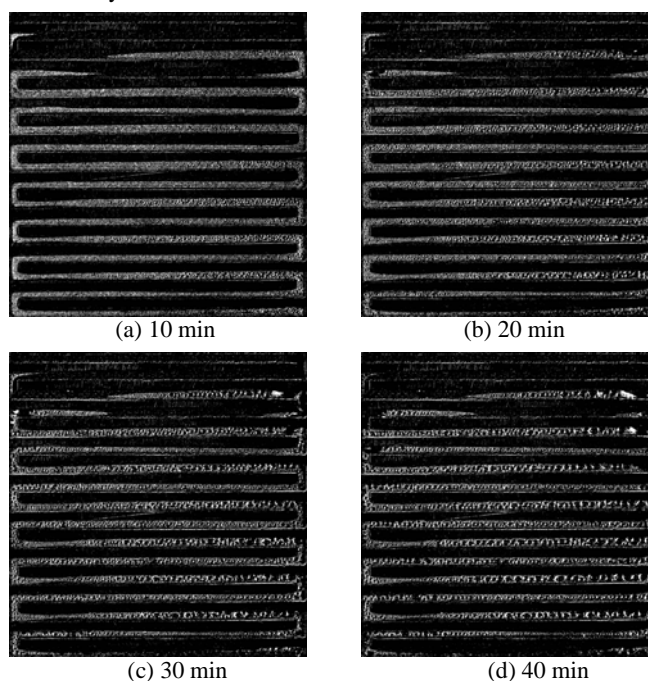
**Figure 8.** Effect of oxygen flow rate on water appearance in cathode flow channel.

Fig. 9. Therefore, the water flooding in a flow channel was more serious at the oxygen stoichiometric ratio of 2.18 because oxygen flow rate was too low to remove the water occurring from the electrochemical sites of the PEM fuel cell. This result corresponds to the study of Weng et al. [14], who reported that water flooding was obvious at a stoichiometric ratio of 2 on the fuel cell operation with dry oxygen flow rate condition. In the case that the oxygen stoichiometric ratio was higher than 3.81, there is not enough water content to keep the membrane in hydrate state according to the experimental result on the oxygen stoichiometric ratio of 15.24 which provided the lowest cell performance as shown in Fig. 10. In this case, since the oxygen gas has not been humidified before entering the fuel cell, the generated water's effect on fuel cell operation was insignificant. So, an appropriate amount of oxygen flow rate must be supplied to remove the excess liquid water out of the cathode flow channel, but still some water remained for fuel cell operation.



**Figure 9.** The water coverage area in cathode flow channels with different oxygen flow rates.

It is important to note that the water coverage area at the oxygen stoichiometric ratio of 3.81 is less than that at 8.16, as shown in Fig. 9. However, this result contradicts the study of water-flooding behavior in cathode flow channel by Weng et al. [14], who reported that the liquid water was easily removed at a high cathode gas flow rate and the reaction area was not hindered by flooding. To explain this experimental deviation, the image processing technique has a limited ability to detection some



**Figure 11.** Effect of operation time on cathode water build-up in the flow field channels.

transparency droplets [12] so that the quantified water coverage area at oxygen stoichiometric ratio of 3.81 was less than the real existent water accumulated in the cathode flow channel. This limitation made reduce the water content at oxygen stoichiometric ratio of 3.81 less than at that 8.16. However, this problem of limited detection of transparency droplets can be corrected by edge detection techniques [22], which will be presented in a future report. Otherwise, the effect of the remaining water as mentioned before in section 4.1 was less dominant on the water content in this deviation case because the fuel cell was operated in the constant temperature with a higher oxygen flow rate.

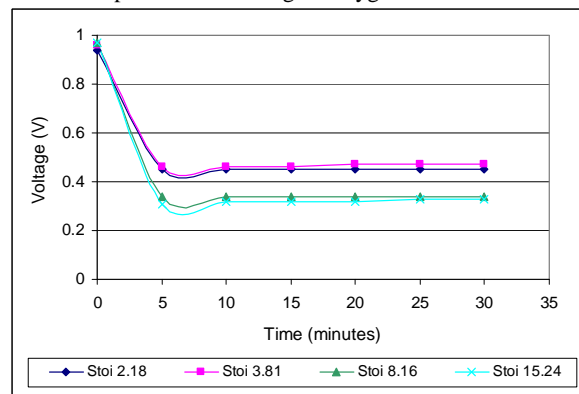


**Figure 10.** The cell voltage in difference oxygen flow rates at a constant current loading of 5 A.

#### 4.3 Effect of fuel cell operation time

The water generation occurred continuously as the fuel cell was in operation. It was monitored and recorded by digital camera regardless of temperature and oxygen flow rate. A transparent PEM fuel cell was loaded at a constant current of 5 A, constant cell temperature of 50°C, non-humidified reactant gases and atmospheric pressure condition. The oxygen gas flow rate was 40 ml min<sup>-1</sup> (stoichiometric ratio of 2.18) and the hydrogen flow rate was 60 ml min<sup>-1</sup> (stoichiometric ratio of 1.63). Fig. 11 shows the processed images of liquid water in the transparent cathode flow channel at different times. All images were recorded at 10 minutes, 20 minutes, 30 minutes and 40 minutes at constant current loading.

It was observed that the small water droplets condensed on the inner surface of transparent acrylic after current loading for 10 minutes. Between 20 minutes and 40 minutes of the fuel cell's operation, the water droplets increased in size and accumulated in the flow channel. The quantification of water coverage area different at times is shown in Fig. 12. The water coverage area in the cathode flow channel decreased gradually while the water droplets increased in size after 20 minutes of operation. Due to a single-serpentine flow field pattern being used in this research, as the Reynolds number was higher than with multiple serpentine channels at the same oxygen flow rate because the flow rate per cross section of a single channel was higher [12] and also because the fuel cell was assembled in a single cell configuration. It was easy to drive the large size of water droplets in the cathode flow channel under an oxygen stoichiometric ratio of 2.18. Thus, water flooding in the transparent cathode flow channel was not observed and the fuel cell performance curve did not show any signal of voltage drop during fuel cell operation time within 40 minutes as shown in Fig. 13. At this steady state (constant voltage), the fuel cell was operated at the same balanced conditions. In spite of the water content declining continuously as shown in Fig. 12, it still maintained the ionic conductivity of the membrane to keep the fuel cell's performance constant. The effect of the fuel cell's operating time was also discussed by Liu et al. [13], who reported that the fuel cell operated at a constant voltage within the first period of operating time (about 30–40 minutes) before the voltage was dropped to a new balanced operating condition at a further period of operating time. However, the steady state in this study was maintained for a longer period than Liu et al. [13] had reported because the fuel cell was operating at a lower current density.

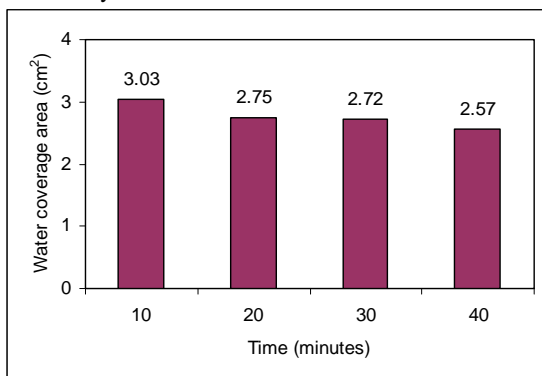


**Figure 12.** The water coverage area on different fuel cell operating time in cathode flow channel.

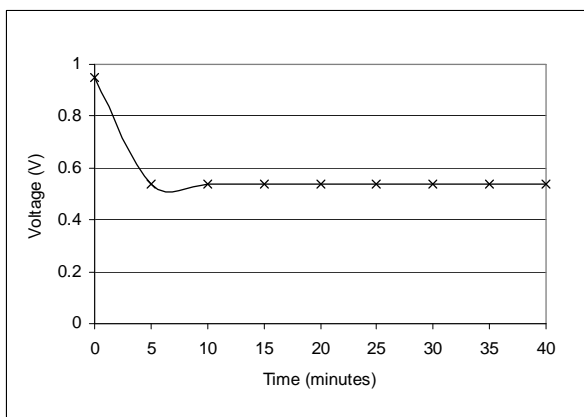


**Figure 13.** The cell performance during operation of a transparent single-serpentine PEM fuel cell.

## 5. Conclusion

The present study has explored the possibility of using image processing techniques to quantify the water content in terms of water coverage area on the cathode flow channel of a PEM fuel cell. Quantification of water coverage area in the cathode flow channel is critical to establishing a basic understanding of the two-phase flow and flooding occurrence in PEM fuel cells. The effect of cell temperature, oxygen flow rates and time development on the water flooding, were analyzed by direct visualization in a transparent single-serpentine cathode flow channel. The digital images from cathode flow channel were recorded to quantify the water coverage area at different operating conditions by using image processing routines. The processed images provided information about the water flooding at different fuel cell operating conditions as follows:

(1) The image of the water at the lowest cell temperature of 25°C shows there was a lot of water coverage area in the cathode flow channel. This could lead to mass transfer limitation because the condensation of the liquid water stays in the channel and occupies the path of the gas to the reaction sites. However, at the highest cell temperature of 70°C, there was insufficient water content to humidify the membrane in the hydrated state. Thus, excessive low or high temperature can lead to deterioration of the fuel cell's performance. The appropriate cell temperature was in the moderate range of 40–60°C, which provided the higher performance.

(2) The cathode gas flow rate can contribute to water removal. By increasing the stoichiometric cathode flow rate from, ratio of 2.18 to 3.81, the water content accumulated in the cathode flow channel can be reduced by almost fifty percent and also lead to higher cell performance. In this study, the reactant was not humidified. When the stoichiometric ratio of oxygen reached 8.16, the cell's performance decreased with the lowest performance at the oxygen stoichiometric ratio of 15.24, because the membrane had become too dry and its conductivity to proton ions had been reduced.

(3) The time development of water flooding did not affect on the cell's performance and the water flooding did not appear in the single-serpentine cathode flow channel. In spite of the water coverage area in the cathode flow channel slightly decreasing within 40 minutes, this water content was able to maintain the ionic conductivity of the membrane to keep the fuel cell operating at the same balanced conditions.

Despite their initial promise, image processing techniques require much more development and refinement for application to a PEM fuel cell. A further development of edge detection techniques, and also, improvements in the resolution of image and photography technique would increase the accuracy of this study.

## Acknowledgements

The author would like to acknowledge the following supporters of this study; Department of Mechanical Engineering, Faculty of Engineering, Chiang Mai University; The Graduate School, Chiang Mai University and Energy Policy and Planning Office, Ministry of Energy, Thailand.

## References

- [1] Chalk SG, Milliken JA, Miller JF, The US Department of Energy – investing in clean transport, *Journal of Power Sources* 71 (1998) 26-35.
- [2] Mehta V, Cooper JS, Review and analysis of PEM fuel cell design and manufacturing, *Journal of Power Sources* 114 (2003) 32–53.

- [3] Pasaogullari U, Wang CY, Liquid Water Transport in Gas Diffusion Layer of Polymer Electrolyte Fuel Cells, *Journal of Electrochem. Soc.* 151 (2004) A339.
- [4] Miachon PA, Internal hydration H<sub>2</sub>/O<sub>2</sub> 100 cm<sup>2</sup> polymer electrolyte membrane fuel cell, *Journal of Power Sources* 56 (1995) 31-36.
- [5] Trung VN, Ralph EW, Water and Heat Management Model for Proton-Exchange-Membrane Fuel Cells, *J. Electrochem. Society* 140 (1993) 2178-2186.
- [6] Springer TE, Wilson M, Gottesfeld S, Modeling and experimental diagnostic in polymer electrolyte fuel cells, *J. Electrochem. Society* 114 (1993) 3513-3526.
- [7] Springer TE, Zawodzinski TA, Gottesfeld S, Polymer electrolyte fuel cell model, *J. Electrochem. Society*, 138 (1991) 2334-2342.
- [8] Yang TH, Yoon YG, Kim CS, Kwak SH, Yoon KH, A novel preparation method for a self-humidifying polymer electrolyte membrane, *Journal of Power Sources* 106 (2002) 328-332.
- [9] Kwaka SH, Yang TH, Kimb CS, Yoona KH, The effect of platinum loading in the self-humidify polymer electrolyte membrane on water uptake, *Journal of Power Sources* 118 (2003) 200-204.
- [10] Hakenjos A, Muentner H, Wittstadt U, Hebling C, A PEM fuel cell for combined measurement of current and temperature distribution, and flow field flooding, *Journal of Power Sources* 131 (2004) 213-216.
- [11] Li H, Tang Y, Wang Z, Shi Z, Wu S, Song D, Zhang J, Fatih K, Zhang J, Wang H, Liu Z, Abouatallah R, Mazza A, A review of water flooding issue in the proton exchange membrane fuel cell, *Journal of Power Sources* 178 (2008) 103-117.
- [12] Spermjak D, Prasad AK, Advani SG, Experimental investigation of liquid water formation and transport in a transparent sing-serpentine PEM fuel cell, *Journal of Power Sources* 170 (2007) 334.
- [13] Liu X, Guo H, Ma C, Water flooding and two-phase flow in cathode channels of proton exchange membrane fuel cells, *Journal of Power Sources* 156 (2006) 267-280.
- [14] Weng FB, Su A, Hsu C-Y, Lee C-Y, Study of water-flooding behaviour in cathode channel of a transparent proton-exchange membrane fuel cell, *Journal of Power Sources* 157 (2006) 674- 680.
- [15] Ous T, Arcoumanis C, Visualisation of water droplets during the operation of PEM fuel cells, *Journal of Power Sources* 173 (2007) 137-148.
- [16] Pekula N, Heller K, Chuang PA, Turhan A, Mench MM, Brenizer JS, Ünlü K, Study of water distribution and transport in a polymer electrolyte fuel cell using neutron imaging, *Nuclear Instruments and Methods in Physics Research, Section A: Accelerators, Spectrometers, Detectors and Associated Equipment* 542/1-3 (2005) 134-141
- [17] Sinha PK, Halleck P, Wang CY, Quantification of liquid water saturation in a PEM fuel cell diffusion medium using X-ray microtomography, *Electrochemical and Solid-State Letters* 9/7 (2006) A344-A348.
- [18] Tsushima S, Teranishi K, Hirai S, Magnetic resonance imaging of the water distribution within a polymer electrolyte membrane in fuel cells, *Electrochemical and Solid-State Letters* 7/9 (2004) A269-A272.
- [19] Yoon W, Huang X, Fazzio P, Reifsnider KL, Akkaoui MA, Evaluation of coated metallic bipolar plates for polymer electrolyte membrane fuel cells, *Journal of Power Sources* 179 (2008) 265-273.
- [20] Tawfik H, Hung Y, Mahajan D, Metal bipolar plates for PEM fuel cell-A review, *Journal of Power Sources* 163 (2007) 755-767.
- [21] Larminie J, Dicks A, *Fuel Cell Systems Explained* (2000) Wiley, West Sussex, England, pp. 69-81
- [22] McAndrew A, *Digital Image Processing with MATLAB* (2004) Course Technology, a division of Thomson Learning, Inc, United States of America, pp. 229